HHS Public Access

Author manuscript

Bone. Author manuscript; available in PMC 2024 September 01.

Published in final edited form as:

Bone. 2023 September ; 174: 116833. doi:10.1016/j.bone.2023.116833.

Muscle secreted factors enhance activation of the PI3K/Akt and β-catenin pathways in murine osteocytes

N. Lara-Castillo[a,*], **J. Masunaga**[a], **L. Brotto**[b], **J.A. Vallejo**[a,c], **K. Javid**[a], **M.J. Wacker**[c], **M. Brotto**[c], **L.F. Bonewald**[d], **M.L. Johnson**[a]

[a]Department of Oral and Craniofacial Sciences, UMKC School of Dentistry, 650 East 25th Street, Kansas City, MO 64108, United States of America

[b]Bone-Muscle Research Center, College of Nursing and Health Innovation, University of Texas at Arlington, 411 S. Nedderman Dr, Arlington, TX 76019, United States of America

[c]Department of Biomedical Sciences, UMKC School of Medicine, 2411 Holmes, Kansas City, MO 64108, United States of America

[d]Indiana Center for Musculoskeletal Health, Barnhill Drive, Indianapolis, IN 46202, United States of America

Abstract

Skeletal muscle and bone interact at the level of mechanical loading through the application of force by muscles to the skeleton. Recently considerable focus has been placed on signaling factors/molecules produced by these two tissues that may act to modulate the function of the other tissue. We sought to determine if muscle and muscle-derived factors were essential to the osteocyte response to loading. Botox® induced muscle paralysis was used to investigate the role of muscle contraction during in vivo tibia compression loading. 5–6 month-old female TOPGAL mice had their right hindlimb muscles surrounding the tibia injected with either BOTOX® or saline. At four days post injections when muscle paralysis peaked, the right tibia was subjected to a single session of in vivo compression loading at ~2600 με. At 24 h post-load we observed a 2.5-fold increase in β-catenin signaling in osteocytes in the tibias of the saline injected mice, whereas loading of tibias from Botox® injected mice failed to active β-catenin signaling in osteocytes. This suggests that active muscle contraction produces a factor(s) that is necessary for or conditions the osteocyte's ability to respond to load. To further investigate the role of muscle derived factors, MLO-Y4 osteocyte-like cells and a luciferase based β-catenin reporter

*Corresponding author at: Department of Oral and Craniofacial Sciences, UMKC School of Dentistry, 650E. 25th Street, Kansas City, MO 64108, United States of America. laran@umkc.edu (N. Lara-Castillo).

Declaration of competing interest

All authors on this manuscript state that they have no conflict of interest with any of the content.

CRediT authorship contribution statement

N. Lara-Castillo: Data curation, Formal analysis, Methodology, Writing – original draft, Writing – review & editing, Project administration, Supervision. **J. Masunaga:** Formal analysis. **L. Brotto:** Formal analysis. **J.A. Vallejo:** Formal analysis, Writing – review & editing. **K. Javid:** Formal analysis. **M.J. Wacker:** Conceptualization, Funding acquisition, Resources, Supervision, Writing – original draft, Writing – review & editing. **M. Brotto:** Conceptualization, Funding acquisition, Supervision, Writing – review & editing. **L.F. Bonewald:** Conceptualization, Funding acquisition, Resources, Writing – review & editing. **M.L. Johnson:** Conceptualization, Data curation, Formal analysis, Project administration, Supervision, Writing – original draft, Writing – review & editing.

(TOPflash-MLO-Y4) cell line we developed were treated with conditioned media (CM) from C2C12 myoblasts (MB) and myotubes (MT) and ex vivo contracted Extensor Digitorum Longus (EDL) and Soleus (Sol) muscles under static or loading conditions using fluid flow shear stress (FFSS). 10 % C2C12 myotube CM, but not myoblast or NIH3T3 fibroblast cells CM, induced a rapid activation of the Akt signaling pathway, peaking at 15 min and returning to baseline by 1–2 h under static conditions. FFSS applied to MLO-Y4 cells for 2 h in the presence of 10 % MT-CM resulted in a 6–8 fold increase in pAkt compared to a 3–4 fold increase under control or when exposed to 10 % MB-CM. A similar response was observed in the presence of 10 % EDL-CM, but not in the presence of 10 % Sol-CM. TOPflash-MLO-Y4 cells were treated with 10 ng/ml Wnt3a in the presence or absence of MT-CM. While MT-CM resulted in a 2-fold activation and Wnt3a produced a 10-fold activation, the combination of MT-CM + Wnt3a resulted in a 25-fold activation of β-catenin signaling, implying a synergistic effect of factors in MT-CM with Wnt3a. These data provide clear evidence that specific muscles and myotubes produce factors that alter important signaling pathways involved in the response of osteocytes to mechanical load. These data strongly suggest that beyond mechanical loading there is a molecular coupling of muscle and bone.

Keywords

Bone-muscle interactions; Wnt/β-catenin; Osteocytes; Fluid flow shear stress; Mechanical loading

1. Introduction

Musculoskeletal diseases represent a huge financial burden to the United States Health Care System and are a leading cause of disability [1]. Osteoporosis (low bone mass and increased skeletal fragility) and sarcopenia (reduced muscle mass and functional deficits) are major contributors to this health care burden. Mechanical loading, such as low and high impact exercise or whole-body vibration, increases both bone and muscle mass in humans [2,3]. Unloading conditions such as bed rest [4,5] and space flight [6] decrease bone and muscle mass significantly. The fact that both bone and muscle show similar effects due to changes in load environment suggests a functional relationship between these tissues. A similar interrelationship has also been observed in pathological conditions such as osteoporosis and sarcopenia, which are highly concordant in the aging population [7,8] and studies have reported a high prevalence of sarcopenia in women who have suffered hip fracture [9]. What is not understood presently is whether one condition precedes the other.

While the traditional view of the muscle-bone relationship is that skeletal muscle loads bone and bone provides an attachment site for skeletal muscles, it is known that both bone and muscle can function as endocrine organs. For example, the skeleton produces and releases at least two important hormones: osteocalcin and Fibroblast Growth Factor 23 (FGF23), which have effects on liver and kidney, regulating glucose and phosphate metabolism respectively [10–12]. Similarly muscle has been shown to secrete factors called “myokines” [13,14] that have effects on other organs including bone. Among the growing list of myokines are the interleukins (IL) -6, -8, -15, brain-derived neurotrophic factor (BDNF) and leukemia inhibitory factor (LIF) [14–16] fibroblast growth factor 21 (FGF21) [17], follistatin-like-1 [17] and more recently Irisin [18] and BAIBA which is also important for the convertion of

white to brown fat [19]. Our group demonstrated an important role for BAIBA in hindlimb unloading in protecting against bone loss and preserving muscle properties [20] and to be a potential biomarker of osteoporosis in younger women [21]. The production and circulation of these factors raises the possibility for a molecular coupling of bone and muscle beyond the traditional mechanical perspective.

One important bone function that might be a target for muscle derived signaling factors/molecules is the response to mechanical loading. The exact mechanism of how bone cells "sense" mechanical loading is not fully understood, although a number of mechanisms have been proposed to account for various aspects of the biochemical events that occur following the application of load to a bone. For example, based upon studies that demonstrated the causal role of a G171V mutation in the low density lipoprotein receptor related 5 (*LRP5*) gene in the high bone mass (HBM) kindred [22], it was first proposed that LRP5 and the Wnt/β-catenin signaling pathway played a key role in bone's responsiveness to mechanical loading [23–25]. Osteocytes are the most abundant cells in bone (around 95 % of the cell population) and are thought to be the primary mechanosensory cells [26,27]. We demonstrated that the activation of the Wnt/β-catenin signaling pathway in murine osteocytes after axial mechanical loading of the ulna involves prostaglandin E_2 (PGE_2) mediated events and that inhibition of Cox-2 prevented this β-catenin activation [28]. ATP and Ca^{2+} fluxes, nitric oxide (NO) and PGE_2 release are known to occur rapidly in response to mechanical loading of bone/bone cells [26,29–31]. Previously Xia et al reported that the effect of PGE_2 on gap junction hemichannels is mediated by the GSK-3β/β-catenin pathway [32]. Armstrong et al reported the translocation of β-catenin in osteoblasts after mechanical stretching and this activation was estrogen receptor (ER) α-dependent [33]. PGE_2 released by mechanical loading prevents glucocorticoid-induced apoptosis through β-catenin [34]. Other pathways have also been implicated in the response of bone cells to mechanical loading, including the integrins [35–37], Ca^{2+} channels [38,39], the PI3K/Akt pathway [40,41] and the MAPK (Erk-1/-2 and p38) pathway [42,43].

Given the established role of the Wnt/β-catenin pathway in bone/osteocyte response to mechanical loading in this paper we sought to determine the role of contracting muscle in the osteocyte response to loading and whether the presence of factors produced by muscle cells would alter activation of Akt signaling and β-catenin nuclear translocation in the osteocyte-like MLO-Y4 cell line. Our data suggests that specific muscles and muscle cells produce factors modify signaling pathways in the osteocyte, supporting our model of biochemical/molecular crosstalk between cells in these two tissues.

2. Material and methods

2.1. Animals

5- to 7-month-old C57Bl/6N (Taconic Farms) female mice were used to generate muscle conditioned media as previously described [44,45]. We used female TOPGAL (originally obtained from the Jackson Laboratory and maintained in our mouse breeding colony) to study the role of contracting muscles on the in-vivo activation of bone cells due to mechanical loading [46]. The TOPGAL mouse is a β-catenin reporter mouse line that carries three copies of the LEF/TCF consensus binding sites for β-catenin that drive the expression

of the lacZ gene when β-catenin translocates into the nucleus. Cells with active β-catenin signaling can be stained with X-Gal and will turn blue [46]. We used OnabotulinumtoxinA (Botox®®, Allergan) injections to paralyze muscles in the right hindlimb based on published reports from two other groups [47,48]. The muscles of the female TOPGAL mouse hindlimb surrounding the right tibia (lateral gastrocnemius, tibialis anterior, soleus, extensor digitorum longus) were injected with a total of 40 μl each of Botox® at a concentration of 2.5 units/100 μl (1 Unit total per hindlimb) (n = 5 mice). As a control the muscles surrounding the right tibia of a separate group of TOPGAL mice were injected with a 40 μl volume of saline (n = 5). Three days post injection, the right tibia was subjected to a single session of loading with the following settings: 9.5 N (~2600 με), 100 cycles, 2 Hz, 0.1 s insertion. Immediately after loading, mice were returned to their cages. Tibias were collected 24 h post loading, fixed in 4 % PFA for 24 h, and processed for β-galactosidase activity staining as previously described [28]. Tibias were embedded in paraffin and cut in 10 μm thick cross sections. Three sites of analysis were selected through 2–5 mm region proximal to the tibia-fibula junction to determine the effect of loading on activation of osteocyte β-catenin signaling. At each bone site, three to four consecutive sections were analyzed and averaged. Sections were collected on positively charged slides and stained with DAPI (to stain the nucleus). Bright field and fluorescent images were obtained from the same section and counted using ImageJ as previously describe by two independent analysts who were blinded to the samples [28]. In case of large discrepancy in the counts, a third analyst re-counted the slides with major differences (>15 %). Cells showing blue staining in bright field images were counted as activated cells. DAPI counts were interpreted as total cell counts. On average 450–500 osteocytes were counted per cross section. Activated cellcounts were divided by total cell number (stained with DAPI) to obtain the percentage of activated cells. All studies were approved by the UMKC Institutional Animal Care and Use Committee.

2.2. Cell culture

MLO-Y4 osteocyte-like cells were cultured as previously described [49] in 150 cm^2 rat tail collagen coated cell culture treated plastic flasks (Corning Inc., Corning, NY, USA). Cells from passages 29–35 were used, plated onto collagen-coated positive-charged slides at a concentration of 6500 cells/cm^2 and used for experiments at 65–75 % confluence. NIH3T3 cells were cultured as previously described [44]. Multipotent C2C12 cells were cultured as previously described [50–52] in 10 %-FBS containing DMEM and were kept at low density (40–50 %) to maintain their myoblast phenotype and avoid spontaneous myotube differentiation media. For myotube differentiation, C2C12 cells in the myoblast stage were seeded at a density of 6500 cells/cm^2. Once cells reached 70–80 % confluency (usually 2–3 days post-seeding) they were switched to differentiation media (DMEM supplemented with 2.5 % horse serum). Cells were then cultured for several days until multinucleated, contracting myotubes were formed, media was replenished every 2 days. To study the effect of conditioned media from cells at different stage of myoblast to myotube differentiation, after differentiation started (Day 0) media was exchanged daily and collected after 24-hour exposure at the end of day 1, 3, 5, and 6. Conditioned media (MB-CM) was obtained after 24 h of cells being exposed to differentiation media. Myotube conditioned media (MT-CM) was collected on Days 5–8 of culture in the differentiation media. A similar cell number to culture media volume ratio was used in all experiments as previously reported [44].

For the mTOR inhibitor studies on Day 5 of differentiation the MT-CM was collected, aliquoted and frozen. Cell culture media was switched to a 0.1 % BSA-1× Penicillin/Streptomycin (P/S)-containing DMEM collecting media with either 10 μM of mTOR inhibitor Ku-0063794 (Shelleckhchem, Houston, TX) (in this paper referred to as Ku) or equal volume of DMSO. After 24 h, Day 6-MT-CM was collected, cells were carefully washed twice with a small amount differentiation. Washes were removed and 9.6 ml of fresh differentiating media was added to the cell culturing plates. After the Day 6 conditioned media collection, cells were then cultured with fresh media changes every 24 h without Ku inhibitor present. 3–4 random images from each 12 well plate of C2C12 cells photographed at 10X magnification were taken and the number of myotubes per image were counted by two independent observers. The conditioned media collected from Day 6, 7 and 8 from both Day 5 Ku-treated and DMSO-treated MT cultures was tested to determine whether it could activate β-catenin signaling in our TOPflash-MLO-Y4 cells. Prior to use, all collected CM were centrifuged at 500*g* for 5 min at 4 °C to remove cells and cellular debris.

2.3. Pulsatile Fluid Flow Shear Stress (FFSS)

Fluid Flow Shear Stress (FFSS) experiments were performed using the Flexcell® Streamer® Shear Stress Device (Flexcell International) as previously described [31]. The media consisted of 90 % αMEM (2.5 % FBS and 2.5 % CS) and 10 % of either 2.5 % Horse serum containing DMEM/High glucose (blank media) or conditioned media from myoblast or myotubes or Ringer solution conditioned by non-contracted or contracted muscles. Cells were subjected to 2 h of pulsatile fluid flow shear stress (FFSS) at 2 dynes/cm^2 [31] or 2 h of static control (in which cells were removed from their media and moved into a different cell culture plate with a volume equal to the volume used for cells exposed to FFSS) in the presence or absence of conditioned media from C2C12 cells or ex-vivo contracted muscles. At the end of the fluid flow regimen, cells were either immediately lysed with lysis buffer (for total protein extraction) or fixed with 2%PFA/0.2%Triton X-100 for immunocytochemistry analysis or lysed for RNA extraction.

2.4. Ex-vivo muscle preparation and contractility

These studies followed previously established protocols [44,53]. We used intact Extensor Digitorum Longus (EDL) and Soleus (Sol) muscles from female 6–7 month old C57Bl/6 N wild type mice (Taconic Farms). Muscles were hung in the chambers for 30 min, the solution was collected (labeled as non-contracted muscle conditioned media) and new Ringer's solution was added. The muscles were then equilibrated by a 30-min stimulation period at 100 Hz (100 Hz, 500 ms long, 1 ms pulses, every 1 min). During this period the optimal length was determined by adjusting the resting tension of the muscle to achieve the maximal force. Following the equilibration period, muscles were stimulated with frequencies from 1 to 130 Hz to obtain the frequencies of stimulation that produces maximal tetanic force; this slightly varies from muscle to muscle. At the end of the equilibration period the Ringer solution was drained, muscles were washed three times with fresh Ringer solution. To obtain contracted CM, muscles were stimulated with high frequency electrical pulses (T_{max}) that were administered with a periodicity of 1 min for a total of 30 min. This Ringer solution was collected and used as stimulated muscle CM.

2.5. Western blotting

PI3K/Akt pathway activation was determined using western blot analysis to detect active Akt (phospho-Akt) and total Akt in the MLO-Y4 cultures at various time points of incubation with MB-CM, MT-CM and CM from contracted Soleus and EDL muscles. Total protein was quantified using a BCA assay (Pierce Biotechnology, Kit #23225). Equal amounts of protein were mixed with loading buffer and loaded onto a Criterion 10 % stocking polyacrylamide gel (BioRad) and run at constant voltage (160 V) for 1 h. Proteins were transblotted onto a PDVF membrane at constant voltage (60 V) for 2 h at 4 °C. Membranes were blocked with 5 % non-fat milk in TBS-T (TBS + 0.1 % Tween-20) for 1 h. Membranes were cut into two pieces at ~50 kDa marker, the upper piece used to detect the phosphorylated form of Akt (60 kDa) and lower portion to detect GAPDH (37 kDa). Primary antibody was diluted in 3 % BSA/TBS-T at different concentrations: p-Akt (Cell Signaling cat #4060) 1:2000, total Akt (Cell Signaling cat# 2938) 1:1000 dilution and GAPDH (Sigma Aldrich, cat# G9545) 1:10,000. We used a different gel to assess expression of total Akt. Incubation with anti-phospho-Akt antibody and total Akt antibody were performed overnight at 4 °C with constant rocking. Incubation with GADPH antibody solution was performed for 1 h at room temperature. The membranes were washed three times with TBS-T for 5 min each. Donkey anti-rabbit HRP-conjugated (GE Healthcare UK Limited, cat#NA934V) secondary antibody was diluted at 1:3000 in 3%BSA/TBS-T and incubated for 1 h at room temperature. Signal was visualized using LAS-4000 Imaging System (FujiFilm). Band intensity was measured using the Multi Gauge analysis software (Fujifilm).

2.6. Immunostaining to detect β-catenin nuclear translocation

After FFSS or static conditions, MLO-Y4 cells were fixed for 10 min in ice-cold 2 % paraformaldehyde (Alfa Aesar) containing 0.2 % Triton X-100 and then washed 3 times in PBS at room temperature for 10 min each. Slides were then incubated overnight at 4 °C with blocking solution [2.5 % bovine serum albumin (BSA) plus 1 % non-immune donkey serum in PBS]. Primary antibody against the active form of β–catenin (Millipore cat#05–665) (diluted 1:100) was used and cells were incubated overnight with antibody solution at 4 °C. Slides were washed three times with PBS and incubated for 1 h with Cy-3 conjugated donkey anti-mouse antibody (1:200) (Jackson ImmunoResearch Labs cat#715–165-150) Alexa 488 phalloidin (diluted 1:250) (Invitrogen™ cat#A12379) and DAPI (diluted 1:250) (Sigma-Aldrich Chemical Co Cat#D9452). Isotype matched nonimmune antibodies were used as a negative control. Cells were photographed under 40× objective lens using a Nikon E800 microscope equipped with epifluorescence light. At least 5 fields of view were taken per condition. Quantitation of nuclear β-catenin immunostaining was performed as previously described [44,54]. Images for display were obtained using a confocal microscope.

2.7. Construction and selection of TOPflash MLO-Y4 β-catenin reporter cell line

To further interrogate the effects of C2C12 CM on osteocytes we stably transfected the β-catenin reporter vector pGL4.49[*luc2P*/TCF-LEF RE/Hygro] (Promega, Cat # E461A, Madison, WI) into MLO-Y4 cells to create a TOPflash-MLO-Y4 cell line. This vector contains eight copies of the TCF-LEF response element (TCF-LEF RE) driving the

transcription of the luciferase reporter gene *luc2P* (*Photinus pyralis*). This vector also contains an ampicillin resistance gene to allow selection in *E. coli* and a gene for hygromycin resistance allowing selection of stably transfected mammalian cell lines.

The MLO-Y4 cells were seeded at a 5600 cells/cm^2 and allow to attach overnight. The next day, serum-free Opti-MEM medium was mixed with ViaFect™ reagent (Promega cat#E4983) and pGL4.49 Luc2P/TCF-LEF/Hygro vector (Promega) at a ratio of 6:1 (transfection reagent:DNA) and incubated for 20 min. The previously plated MLO-Y4 cells were switched to growth media without antibiotics. An aliquot of the Opti-MEM ViaFect:DNA complex was added to the cells. After two days the transfection media was removed and replaced with growth media containing 300 ng/ml of hygromycin for two weeks with fresh media changes every third day.

Colonies were lifted from the plate using trypsin-soaked sterile filter paper. Cells were then plated onto collagen-coated plates and allowed to expand. Clones were tested for their response to 10 mM lithium chloride (LiCl) and 10 ng/mL Wnt3a. Colonies with the highest response were selected for single cell expansion. Colonies were trypsinized (0.05 % Trypsin-0.53 mM EDTA 1×, Corning) diluted to ~0.5 cells per 100 µl. A 100 µl aliquot of diluted cells was plated into each well of a 96-well plate. After 24 h, wells with a single cell were identified and clones were allowed to divide and expand. Single cell clones were then tested for response to LiCl and Wnt3a. Three clonal cell lines with the highest response were selected and expanded for use in subsequent studies.

2.8. Luciferase assay

The selected TOPflash-MLO-Y4 single-cell clones were tested for their ability to respond to different stimuli using the Luciferase Assay System as described by the manufacturer (Promega, catalog # E1501) per well in a white well Culturplate™-96-well plate (PerkinElmer). 5000 cells per well were seeded in collagen-coated 96-well plate and allowed to attach overnight. Cells were then treated with lithium chloride (10 mM) or different concentrations of Wnt3a (1–100 ng/ml) and incubated for 24 h. The next day cells were washed with DPBS and lysed with 50 µl of Luciferase Cell Culture Lysis Reagent. We took 20 µl of cell lysate and add 100 µl of Luciferase Assay Reagent. L uminescence was measured for 10 s in either a Victor Multi-label Counter or the VICTOR Nivo™ Multimode Plate Reader (both instruments from Perkin-Elmer, CT).

2.9. DNA measurement

To normalize the luminescence, 270 µl of high salt buffer (100 mM Tris-HCl, pH 7.4, 10 mM EDTA, 2 M NaCl) was added to the remaining 30 µl of cell lysate. Plates were subjected to two rounds of freezing/thawing. Total DNA in each well was determined using the DNA Quantitation kit, (Sigma-Aldrich, Cat# DNAQF) according to manufacturer's instruction. 10 µl aliquot of the cell lysate was mixed with 200 µl of the Assay Buffer containing the compound H33258 (Hoechst 33258) at a final concentration of 0.1 µg/ml in a black 96-well plate. [55]. Plate was incubated in the dark for 24 h. Fluorescence measurements were obtained using a VICTOR Nivo™ Multimode Plate Reader (Perkin-

Elmer) at 360 nm for excitation and 460 nm for emission. A standard curve was generated each time using DNA standard (Sigma Aldrich, cat# D4810).

2.10. Statistical analysis

All data were analyzed using the Statistical packages IBM SPSS Statistics 28 and GraphPad Prism 9.1.2. All data were first screened for extreme outliers and values > ±3 standard deviations, were adjusted using winsorization method. Next, data were tested for homogeneity of variance (Levene's test) and normal distribution (Shapiro-Wilk test). For data meeting these requirement we used Student's *t*-test, paired Student *t*-tests or ANOVA to analyze the data. For experiments in which these assumptions were not met, we first applied a log10 transformation. If after transformation the assumptions were met we used a one-way analysis of variance (ANOVA) and post hoc tests for group comparisons. If assumptions were still not met we used a Kruskal-Wallis mean ranks test. Statistical significance was set to alpha level of 0.05.

3. Results

3.1. Contracting muscle is required for mechanical load induced activation of β-catenin signaling in osteocytes

We initially investigated the role of skeletal muscle in the bone response to mechanical loading by paralyzing the right hindlimb muscles surrounding the tibia using Botox® followed by loading at a strain level known to induce activation of β-catenin signaling in osteocytes [28]. As expected [47,48], at 4 days post injection the Botox® injected mice were no longer ambulating on the injected right hindlimb but controls injected with saline could ambulate fine. Shown in Fig. 1A are representative images of the cross sections we counted to determine activation of β-catenin signaling in osteocytes. Fig. 1B shows the results of our counts. The saline injected control mice with fully functional and contracting muscles showed the expected ~2-fold increase in β-catenin signaling in osteocytes at 24 h post load [28]. In animals injected with PBS, the mean percentage of activated cells in non-loaded tibia was 10.81 ± 2.97 % and in the loaded tibia was 20.54 ± 5.46 % (n = 5). In animals injected with Botox® the mean percentage of activated cells in the non-loaded tibia was 7.17 ± 1.62 % and in the loaded tibia was 7.54 ± 1.04 % (n = 5). There was a significant difference in β-galactosidase activated cells in loaded vs non-loaded tibia in the PBS injected mice ($p < 0.01$, n = 5). However, mice in which the surrounding muscles of the loaded right tibia were paralyzed by Botox®, the osteocytes failed to activate the β-catenin signaling pathway ($p = 0.745$, n = 5).

3.2. Muscle secreted factors induce osteocyte β-catenin nuclear translocation

We next investigated whether *ex-vivo* contracting muscles could potentially produce signaling molecules/factors capable of inducing translocation of β-catenin into the nucleus in osteocytes. We generated conditioned media (CM) from ex vivo contracted EDL and Soleus muscles (C57Bl/6 female mice) and tested for the ability of these media to activate MLO-Y4 cells. Based on previous experiments (data not shown) we determined that induction of β-catenin nuclear translocation was observed with 10 % MT-CM but not MB-CM. Therefore, we exposed MLO-Y4 cells to 10 % muscle conditioned media. Fig. 2 shows

the effects of 10 % EDL and 10 % SOL muscle CM on nuclear translocation of β–catenin in static MLO-Y4 cells. We exposed MLO-Y4 to different CM and measured the expression of β-catenin in the different cell compartments then obtain the nuclear/cytoplasmic ratio. The β-catenin nuclear to cytoplasmic ratio in the EDL-CM contracted (1.99 ± 0.47, n = 4) treated group was significantly different ($p < 0.05$) from the Blank (ringer solution) (1 ± 0.08, n = 3), Soleus-CM non contracted (0.94 ± 0.42, n = 3), EDL-CM non contracted (1.19 ± 0.25, n = 3). The effect size was calculated as $\omega 2 = 0.40559$ indicating that ~40.6 % of variance in the ratio of β-catenin nuclear:cytoplasmic was due to the presence of conditioned media from the different muscles and conditions.

3.3. Specific muscle cells secrete factors that activate Akt signaling in MLO-Y4 cells

To further explore the activation of β-catenin in response to conditioned media from C2C12 myotubes and contracted EDL muscle we next examined activation of Akt signaling as a potential upstream activator of β-catenin signaling [28]. MLO-Y4 cells were exposed for 30-minute to CM collected from days 1 through 6 of C2C12 cell differentiation. Cell lysates were analyzed by western blots using antibodies against the phosphorylated form of Akt (Ser493), total Akt, and GAPDH for internal control. There was no difference in total protein during the length in the experiment. Band density was measured and ratio of phospho-Akt to GAPDH was plotted. Mean ranks were statistically significantly different among groups, $H^2(3) = 20.810$, $p < 0.001$. Mean ranks for blank and C2C12 CM from Day 1 were 6.58 (n = 12), for Day 3 = 20.83 (n = 6), Day 5 = 22.5 (n = 6), and Day 6 = 21.0 (n = 6). Subsequently, pairwise comparisons were performed using Dunn's (1964) procedure with a Bonferroni correction for multiple comparisons. This post hoc analysis revealed statistically significant differences in p-Akt/GAPDH ratio between Blank and Day1 vs Day3 ($p = 0.007$), Blank and Day1 vs Day5 ($p = 0.006$), Blank and Day1 vs Day6 ($p = 0.002$) (Fig. 3A). We further explored the kinetics of this activation with conditioned media obtained from myoblasts (MB-CM), myotubes (MT-CM), and fibroblasts (NIH3T3). As observed in Fig. 3B, there was a rapid, but transient increase in Akt phosphorylation as early as 15 min with both the MT-CM and MB-CM, with the MT-CM treatment achieving a higher level of activation. This activation was maintained at 30 min with MT-CM, but not with MB-CM and the activation by MT-CM returned to basal levels after 2 h post initial exposure (Fig. 3B, black arrow). Based on these results, we used CM from day 1 when cells are predominantly in their myoblast stage (MB-CM) and day 6 when cells are in their differentiated myotube stage (MT-CM).

Next the activation of Akt in response to fluid flow shear stress (FFSS) was examined in the presence and absence of MB-CM and MT-CM. There were statistically significant differences in the p-Akt/GAPDH ratio between the groups of static + blank versus FFSS + Blank ($p = 0.018$), static + blank versus FFSS + MT-CM ($p < 0.001$), static + MB-CM versus FFSS + blank ($p = 0.03$), static + MB-CM vs FFSS + MT-CM ($p < 0.001$), static + MT-CM versus FFSS + blank ($p = 0.002$), static + MT-CM versus FFSS + MB-CM ($p < 0.008$), static + MT-CM versus FFSS + MT-CM ($p < 0.001$). (Fig. 3C). To determine if ex vivo contracted primary muscle fibers could also enhance Akt activation in response to FFSS, MLO-Y4 cells were exposed to FFSS for 2 h in the presence of 10 % muscle condition media from Soleus (Sol) or EDL from 5 to 7 months old C57Bl/6 male mice.

Mean ranks were statistically significantly different among groups $H^2(5) = 12.189$, p = 0.032. Mean ranks for the different groups were as follow: Static + Ringer Solution = 1.0, n = 4; Static + Sol-CM = 1.04, n = 4; Static + EDL-CM = 0.512, n = 3; FFSS + Ringer Solution = 3.63, n = 4; FFSS + Sol-CM = 2.74, n = 4; FFSS + EDL-CM = 5.13 n = 4. Shown in Fig. 3D, FFSS + EDL-CM was statistically different from static + Ringer (p = 0.012), static + Sol-CM (p = 0.016), and static + EDL-CM (p = 0.008).

3.4. Synergistic effects of MT-CM and Wnt3a

Three clonal isolates of TOPflash MLO-Y4 cells were obtained from our stable transfection of MLO-Y4 cells with the TOPflash vector. Luciferase activity, driven by the TCF-LEF promoter, is an indicative of β-catenin translocation to the nucleus. As shown in Fig. 4, all three cell lines demonstrated a dose response increase in luciferase activity to increasing amounts of Wnt3a after 24 h of incubation. Clone A3-F9 was selected for further studies due to its lower expression of osteoblast markers (data not shown). We first confirmed the activation of β-catenin signaling in the A3-F9 TOPflash cell line to myotube conditioned media (MT-CM). As shown in Fig. 4B, 10 % MT-CM but not myoblast conditioned media (MB-CM) induced a similar fold increase in β-catenin signaling as was observed in the prior studies (Fig. 2). A one-way ANOVA test was run to determine if addition of 10 % MT-CM would increase luciferase activity in the A3-F9 TOPflash cell line. The mean for the fold change of luciferase activity was 1.03 ± 0.15, n = 3 for the blank group, 0.95 ± 0.3 for the MB-CM group, and 1.94 ± 0.56 for the MT-CM group. Luciferase activity was statistically significantly different between the different groups, p = 0.013. A Least Significant Difference (LSD) Test post hoc analysis determined that luciferase activity was statistically different in cells treated with MT-CM when compared to blank (p =0.017) and MB-CM (p =0.011). The effect size was calculated as $\omega^2 = 0.76$ or ~76 % of the variance in luciferase activity is accounted for by addition of conditioned media. Interestingly, when MT-CM was combined with a submaximal dose of 10 ng/ml of Wnt3a we observed a synergistic effect in the activation of β-catenin signaling in the TOPflash cells (Fig. 4C). The mean ± SD for the blank group was 1.02 ± 0.24, n = 6, for the MT-CM group 3.12 ± 1.27, n = 8, for the Wnt3a group = 16.03 ± 6.02, n = 6, and for the Wnt3a + MT-CM = 39.28 ± 24.92, n = 6. Luciferase activity was statistically significant different between the different groups, p < 0.001. An LSD test post hoc analysis determined that all groups were statistically different among themselves. Most importantly, groups Wnt3a and Wnt3a + MT-CM were statistically different from one another (p = 0.003). The effect size was calculated as $\omega^2 = 0.9115$, indicating that ~91 % of the variance in the luciferase activity was accounted by the addition of treatments. We did not observed this synergistic effect when TOPFlash-MLOY4 cells were incubated with MBCM in combination with Wnt3a (13.3 ± 2.76, n = 2).

3.5. C2C12 cell stimulatory factor production is regulated by mTOR

We next sought to determine what might be regulating the production of this C2C12 myotube factor that synergizes with Wnt3a. C2C12 Myotubes were cultured and treated with 10 μM of the mTOR inhibitor (Ku-0063794) or vehicle on d5 of differentiation for 24 h. Cells were washed three times with DPBS and fresh media was added. Myotube conditioned media (MT-CM) was collected on day 6. Ku-0063794 dramatically reduced the

number of myotubes present in the cultures visible on day 6 after a 24-hour treatment with the mTOR inhibitor (not shown). TOPflash-MLO-Y4 cells were subsequently incubated for 24 h with 10 % of MT-CM from different day of differentiation in the presence or absence of 10 ng/mL Wnt3a. Luciferase activity was measured and for this analysis we measured total DNA in each well. Luciferase activity was divided by total DNA. Fold change in the luciferase activity relative to the blank is reported as mean ± std. deviation. The values for the Wnt3a treatment alone = 20.92 ± 4.42, n = 5, Wnt3a + MT-CM (from day 5) = 27.73, n = 4, Wnt3a + MT-CM (from day 6) = 47.87, n = 5, Wnt3 + MT-CM (from day 6) in the presence of the mTOR inhibitor = 13.13 ± 4.17, n = 4. Luciferase activity was statistically significantly different between the different groups, $p < 0.001$. An LSD post hoc test was performed, and all groups were statistically different against each other with the exception of blank vs MT-CM Day 5. Luciferase activity from cells treated with MT-CM Day 6 was statistically different from blank ($p = 0.002$), MT-CM Day 5 ($p = 0.043$), and MT-CM Day 6 + mTOR inhibitor ($p < 0.001$). Luciferase activity in cells incubated with MT-CM Day 6 + mTOR inhibitor was significantly lower than the blank ($p = 0.043$). The effect size was calculated as $\omega^2 = 0.5335$. Thus, ~53 % of the variance in the luciferase activity was accounted for the addition of treatments.

To determine if the inhibitory effects of the Ku-0063794 on production of the myotube factor was reversible after treatment on day 5 with the inhibitor for 24 h we removed the inhibitor and collected CM from days 6, 7 and 8. As shown in Fig. 5B, synergistic effect by Ku-0063794 (14.36 ± 4.1, n = 3) was statistically significantly different from MT-CM Day 6 without the mTOR inhibitor (54.1 ± 17.31, n = 4) ($p = 0.02$). There was not a difference between cells treated with MT-CM Day 7 and MT-CM Day +Ku-0063794 ($p = 0.119$), and cells treated with MT-CM Day 8 and MT-CM Day 8 + Ku-0063794 ($p = 0.356$). In Fig. 5C we show the percentage of myotubes per field relative to Day 5 of culture (before addition of Ku-0063794 or DMSO). The number of myotubes in culture in Day 6 (73.53 ± 17.24, n = 5, $p = 0.006$), Day 7 (68.27 ± 16, n = 4, $p = 0.043$), Day 8 (61.27 ± 12.26, n = 4, $p = 0.005$) decreased in culture treated with mTOR inhibitor as compared to Day 5 of the same culture before addition of treatment. The percentage of myotubes in DMSO treated did not change across throughout day of culture Day 6 (94.96 ± 11.13, n = 5, $p = 0.583$), Day 7 (81.93 ± 16.16, n = 4, $p = 0.14$), or Day 8 (81.93 ± 16.16, n = 4, $p = 0.124$).

4. Discussion

The importance of muscle-bone molecular/biochemical crosstalk in the functionality of both tissues is now being widely recognized, beyond just the mechanical coupling of skeletal muscle and bone. Mechanical loading of bone is followed by rapid activation of β-catenin signaling in osteocytes [28]. In this study, we paralyzed the muscles surrounding the tibia using Botox® and then subjected the paralyzed hindlimb to in vivo mechanical loading at 3 days post injection when muscle immobilization has been shown to reach its peak [47]. The load/strain magnitude sufficient to activate osteocyte β-catenin signaling [28] and we observed a complete lack of activation in the paralyzed loaded limb. What might explain this observation? Botox® targets the SNARE protein synaptosomal-associated protein 25 (SNAP-25) regulating the release of acetylcholine into the neuromuscular junction [56]. One possibility is that the Botox® had a direct effect on bone through its muscarinic

acetylcholine receptors rather than acting through muscle. Gehling et al demonstrated that injection volumes of 25 and 50 μl remained in the injection site of the mouse caudal thigh muscle [57]. Furthermore, Tang-Liu et al. demonstrated that 70 units of radiolabeled Botox® did not diffuse away from the injection site [58]. Given that we injected a total of 40 μl (1unit) into the belly of all hindlimb muscles of these TOPGAL mice, it seems highly unlikely that these findings could be explained by leakage of the Botox® out of the injection sites and some direct effect on bone. The response to a single bout of mechanical loading has been shown to be neuronally regulated [74]. Interestingly, studies by two groups [75,76] have shown that Botox® induced muscle paralysis under normal ambulation differentially alters cancellous versus cortical bone in the paralyzed limb. Bain et al. [75] concluded that neuromuscular signaling functioned independently from mechanical loading and particularly modulated trabecular bone homeostasis. An alternative possible neural explanation might be an effect of Botox® on altered proprioception [77] leading 22 to a central level mediated altered response of bone to mechanical loading. The role of proprioception involving afferent nerves has not been examined in the context of mechanical loading of bone. Studies have shown that specific neurons in the brain such as those found in the arcuate nucleus can influence bone properties [78,79]. Whether a feedback loop exists between muscle proprioception nerves and the brain (or CNS) and then to bone to regulate the response to mechanical loading has not been explored to the best of our knowledge. Our studies demonstrating that ex vivo contracted muscles and C2C12 myotube conditioned media can activate β-catenin signaling in MLO-Y4 cells suggests a direct effect of a signaling molecule produced by specific muscle fibers is acting on bone as this in vitro model lacks a neural component.

Another possibility is that after 4-days of Botox® induced “unloading” in the paralyzed limb the osteocytes have become refractory to load stimuli and need to be primed to respond by multiple loading sessions. Alternatively, higher load magnitudes are needed to activate β-catenin signaling in the Botox® treated hindlimb. Holguin, Brodt and Silva reported that a single loading session or 5 days of loading produced a similar amount of activation of TOPGAL-expressing osteocytes in 5-month-old TOPGAL mice [80]. Also, they did not observe a significant difference between the two magnitudes of load (650 or 2200 με) used in the 5-month-old TOPGAL mice. We used a slightly higher magnitude of load (~2,600με) so it would seem that increasing the magnitude of load might not result in osteocyte activation of the paralyzed limb. Further studies are needed to determine if multiple loading sessions would result in activation of β-catenin signaling in the Botox® treated hindlimb. Qin and Lam demonstrated that stimulation of the quadriceps of a hindlimb suspended rat could rescue the bone loss observed in non-stimulated limbs [59,60]. They proposed that muscle contraction resulted in fluid pressure gradients in the bone that would stimulate bone formation. Similarly Swift et al. [61] showed that high-intensity muscle contractions could prevent the loss of muscle strength and stimulate bone formation due to hindlimb unloading. Our Botox® induced muscle immobilization studies provide further evidence in support of the need for a contracting muscle to support β-catenin signaling in osteocytes in response to loading. We have previously shown that β-catenin mediated signaling in bone (osteocytes) is required for new bone formation in response to mechanical loading [62]. While our loading of a Botox® immobilized tibia should provide an increase in fluid pressure (flow)

in bone, if contracting muscle is required for only this mechanical aspect, then we would have expected to observe activation of β-catenin signaling in osteocytes by the mechanical loading we applied, which did not occur. Studies with hindlimb immobilization have shown that the muscle secreted factor L-BAIBA protects against osteocyte apoptosis in the murine hindlimb unloading model [20]. Furthermore, the role of the musculoskeletal secretome and its regulation by exercise induced muscle contraction and bone loading is emerging as an important concept in the maintenance of bone and muscle mass and function (see Reviews [63–65]). We therefore interpret our current in vivo loading studies as supporting the concept that a contracting skeletal muscle produces factors that condition or facilitate the osteocyte's ability to respond to mechanical loading of bone.

We have previously shown that L-BAIBA provided in the drinking water of hindlimb suspended mice can protect against disuse associated bone loss [20]. Unfortunately, the TOP*flash*-MLO-Y4 cell line we created does not express the Mas-Related G protein-coupled Receptor Type D (Mrgprd) receptor [20] that binds L-BAIBA, so we were not able to directly test this myokine in our in vitro system. Instead, we chose to further examine the role of muscle derived factors in the activation of β-catenin signaling in the osteocyte by using conditioned media from the C2C12 myoblast/myotube cell line and ex vivo contracted EDL and Soleus muscles to treat the MLO-Y4 osteocyte-like cells. We found that conditioned media from C2C12 myotubes and contracted EDL muscle contain unknown factors that are capable of transiently activating the PI3K/Akt signaling pathways in our osteocyte models independent of mechanical loading (fluid flow shear stress) and increase activation of this pathway in the presence of mechanical loading. Activation of these pathways are known to be important in mediating the response of bone to mechanical loading [24,28,40,41,66–68]. The potency of the MT-CM for activation of Akt signaling peaked by Day 3 of myotube differentiation and was maintained up to day 7. Day 1 MB-CM showed ~1/2 the level of Akt activation at 15- and 30-min relative to day 6 MT-CM. We suspect this is due to the presence of a low amount of myotube formation that occurs within 24 h of inducing differentiation in the C2C12 cultures. The kinetics of Akt activation indicate a rapid activation and return to baseline by 2 h of incubation in the presence of MT-CM and a return to baseline by 1 h of incubation with MB-CM. Subsequent studies used a 2-h incubation timepoint for our CM studies. Conditioned media from fibroblast cell line, NIH3T3, did not have the same effect. These results in combination with other work from our lab [44] support the hypothesis that muscle biochemically crosstalks with bone (osteocytes) and that this is potentially part of an endocrine/paracrine loop driving key molecular/biochemical signaling pathways between these two intimately associated tissues.

Our newly developed TOPflash-MLO-Y4 cell line showed activation of the Wnt/β-catenin pathway in the presence of myotube, but not myoblast, conditioned media after 24 h of incubation (Fig. 4B). Surprisingly, when we combined both MT-CM and a 10 ng/ml dose of Wnt3a, which sub-optimally activates β-catenin signaling in the TOPflash-MLO-Y4 cells we observed a significant synergistic activation of the pathway. Given that MT-CM by itself only activates β-catenin signaling in these cells ~2–3 fold, we interpret this to suggest that the factor produced by the myotubes is not a Wnt protein, but some other factor. If, for example, this factor is a high concentration of a Wnt protein, then we would have expected a much higher activation by MT-CM alone as observed in the dose response to added Wnt3a

in our TOPflash-MLO-Y4 cells. This exciting observation raises the question of what is this factor(s) that is being produced by myotubes? Since our TOPflash-MLO-Y4 cell line does not express the Mrgprd receptor this would argue that L-BAIBA is not one of the possible factors that might be present in these conditioned medias that could account for this synergistic effect.

Fluid flow shear stress (FFSS) and PGE_2 are known to induce β-catenin nuclear translocation in osteoblast-like and osteocyte-like cells [32,66,69,70]. Myotube conditioned media triggered β-catenin nuclear translocation under static conditions in the MLO-Y4 osteocyte-like cells and primary osteocyte enriched cell populations. [71] Here we have shown that conditioned media from contracted EDL muscle (EDL-CM) was able to induce nuclear translocation of β-catenin (Fig. 2). C2C12 MT-CM, but not NIH3T3 fibroblast CM, was able to transiently increase phosphorylation of Akt in the MLO-Y4 cells under static conditions; peaking at about 30 min and then returning to baseline by 2 h (Fig. 2C). The duration of Akt activation was prolonged when MT-CM and EDL-CM was used, suggesting that muscle cells CM contains a factor (or factors) that acutely and transiently activate the PI3K/Akt pathway. We have previously shown that the PI3K/Akt signaling pathway is activated by FFSS [28]. When MLO-Y4 cells were subjected to FFSS in the presence of myotube CM and EDL-CM, we observed a synergistic activation of the PI3K/Akt pathway, but not with C2C12 myoblast CM or Soleus CM. Interestingly, when MLO-Y4 cells were subjected to FFSS in the presence of the different muscle cells CMs, we did not observe further increases in β-catenin nuclear translocation compared to FFSS alone. This could be due to the relative insensitivity of our method for quantitating β-catenin nuclear translocation or perhaps suggests that the response to FFSS has reached a maximum. To explore this further we will need to test lower levels of FFSS.

The stimulatory effect of EDL CM vs Soleus CM could be due to several factors. The EDL is a fast twitch glycolytic and more fatigable muscle, and the Soleus is a slow twitch, oxidative and more resistant to fatigue muscle. The EDL muscle is mainly composed of fibers type II (b and x) and the Soleus is mainly integrated by fibers type I and IIa. As we age the percentage of the total muscle cross-sectional area occupied by fiber type I tend to increase [72,73] and type II fiber types as well as cross sectional area tend to decrease; therefore it will be very interesting to determine if the observed activation is lost when aged muscle are contracted.

In an attempt to better understand the mechanism regulating the production of this myotube produced factor several signaling pathways were studied. Among these was the mTOR pathway. When C2C12 were treated with Ku-0063794, a mTORc2 inhibitor, production of the muscle factor(s) that activates β-catenin in osteocyte was lost. This suggest that mTOR signaling in muscle cells is involved in the production of the factor(s). The inhibition of the production of muscle factors was transitory.

Our studies have some limitations. We need to more fully dissect the mechanism of action of Botox® on loading induced activation of β-catenin signaling in osteocytes. Our ultimate goal is to identify the muscle derived signaling molecules/factors involved in muscle-bone crosstalk and these studies are currently underway using a variety of proteomic, lipidomic,

proteomic and metabolomic approaches of serum and conditioned media. The TOPflash MLO-Y4 cell line we created did not express the Mrgprd receptor, therefore we were not able to directly test L-BAIBA in our osteocyte cell culture model system. However, it should be possible to test this in vivo by providing L-BAIBA in the drinking water of the Botox® immobilized mice. Since we only tested 27 muscles from female mice, it will also be of interest to determine if there are male versus female differences in terms of the production of these signaling factors/molecules once they are identified and if/how these factors may contribute to sex differences in muscle and bone. Finally, understanding the regulation of this muscle derived factor relative to aging and estrogen loss that occurs during menopause in humans will be important to determine as these conditions are central to understanding bone loss and muscle function deficits in humans that accompany these changes.

In conclusion we present compelling data that supports the hypothesis that muscle cells, in vitro and ex vivo, secrete factors that are able to act on osteocytes altering the Wnt/β-catenin, mTOR and PI3K/Akt signaling pathways. Further studies aim to identify the factor(s) in muscle CM responsible for this pathway regulation are currently underway. The identification of these factor(s) could provide a new therapeutic target/paradigm for enhancing the effects of loading (exercise) on the skeleton, especially if these factor(s) are diminished with aging and this accounts for the well-known loss of effectiveness of exercise on the skeleton that occurs with aging.

Acknowledgements

The authors thank Julia Karabilo for her help with the CM pilot studies. *Author's role*: NL-C performed most of the experimental work, organization and analysis of the data, and primary writing of the manuscript; JM performed the mTOR inhibitor studies; LB, JV and MW provided muscle conditioned media and helped with writing the manuscript; MB and LFB provided concepts, support and help in writing of manuscript; KJ analyzed the Botox® data; MLJ provided concept, experimental design, overall supervision of project and writing of manuscript. All authors have reviewed and accepted the data in the manuscript. The Graphical Abstract was created with BioRender.com.

Funding

The project was funded by a grant from the National Institutes of Health PO1AG039355 to LB, MW, MB and MLJ and a minority supplement NIA 3P01AG039355-08S2 to JV. JM was supported by the UMKC School of Dentistry Summer Scholars Program.

Data availability

Data will be made available on request.

References

[1]. Yelin E, Cost of musculoskeletal diseases: impact of work disability and functional decline, J. Rheumatol. Suppl. 68 (2003) 8–11. [PubMed: 14712615]

[2]. Vainionpaa A, et al. , Effect of impact exercise and its intensity on bone geometry at weight-bearing tibia and femur, Bone 40 (3) (2007) 604–611. [PubMed: 17140871]

[3]. Reyes ML, et al. , High-frequency, low-intensity vibrations increase bone mass and muscle strength in upper limbs, improving autonomy in disabled children, J. Bone Miner. Res. 26 (8) (2011) 1759–1766. [PubMed: 21491486]

[4]. Donaldson CL, et al. , Effect of prolonged bed rest on bone mineral, Metabolism 19 (12) (1970) 1071–1084. [PubMed: 4321644]

[5]. Vico L, et al. , Effects of a 120 day period of bed-rest on bone mass and bone cell activities in man: attempts at countermeasure, Bone Miner. 2 (5) (1987) 383–394. [PubMed: 3146359]

[6]. Collet P, et al. , Effects of 1- and 6-month spaceflight on bone mass and biochemistry in two humans, Bone 20 (6) (1997) 547–551. [PubMed: 9177869]

[7]. Frontera WR, et al. , Skeletal muscle fiber quality in older men and women, Am. J. Physiol. Cell Physiol. 279 (3) (2000) C611–C618. [PubMed: 10942711]

[8]. Visser M, et al. , Change in muscle mass and muscle strength after a hip fracture: relationship to mobility recovery, J. Gerontol. A Biol. Sci. Med. Sci. 55 (8) (2000) M434–M440. [PubMed: 10952365]

[9]. Di Monaco M, et al. , Prevalence of sarcopenia and its association with osteoporosis in 313 older women following a hip fracture, Arch. Gerontol. Geriatr. 52 (1) (2011) 71–74. [PubMed: 20207030]

[10]. Aono Y, et al. , Therapeutic effects of anti-FGF23 antibodies in hypophosphatemic rickets/osteomalacia, J. Bone Miner. Res. 24 (11) (2009) 1879–1888. [PubMed: 19419316]

[11]. Yoshiko Y, et al. , Mineralized tissue cells are a principal source of FGF23, Bone 40 (6) (2007) 1565–1573. [PubMed: 17350357]

[12]. Lee NK, et al. , Endocrine regulation of energy metabolism by the skeleton, Cell 130 (3) (2007) 456–469. [PubMed: 17693256]

[13]. Pedersen BK, et al. , Role of myokines in exercise and metabolism, J. Appl. Physiol. 103 (3) (2007) 1093–1098. [PubMed: 17347387]

[14]. Pedersen BK, Febbraio M, Muscle-derived interleukin-6—a possible link between skeletal muscle, adipose tissue, liver, and brain, Brain Behav. Immun. 19 (5) (2005) 371–376. [PubMed: 15935612]

[15]. Febbraio MA, Pedersen BK, Muscle-derived interleukin-6: mechanisms for activation and possible biological roles, FASEB J. 16 (11) (2002) 1335–1347. [PubMed: 12205025]

[16]. Pedersen BK, Febbraio MA, Muscle as an endocrine organ: focus on muscle-derived interleukin-6, Physiol. Rev. 88 (4) (2008) 1379–1406. [PubMed: 18923185]

[17]. Izumiya Y, et al. , FGF21 is an Akt-regulated myokine, FEBS Lett. 582 (27) (2008) 3805–3810. [PubMed: 18948104]

[18]. Colaianni G, Grano M, Role of Irisin on the bone-muscle functional unit, Bonekey Rep. 4 (2015) 765. [PubMed: 26788285]

[19]. Boström P, et al. , A PGC1-α-dependent myokine that drives brown-fat-like development of white fat and thermogenesis, Nature 481 (7382) (2012) 463–468. [PubMed: 22237023]

[20]. Kitase Y, et al. , beta-aminoisobutyric acid, l-BAIBA, is a muscle-derived osteocyte survival factor, Cell Rep. 22 (6) (2018) 1531–1544. [PubMed: 29425508]

[21]. Wang Z, et al. , Quantification of aminobutyric acids and their clinical applications as biomarkers for osteoporosis, Commun. Biol. 3 (1) (2020) 39. [PubMed: 31969651]

[22]. Akhter MP, et al. , Bone biomechanical properties in Lrp5 mutant mice, Bone 35 (2004) 162–169. [PubMed: 15207752]

[23]. Akhter MP, et al. , Effects of a mutation in the Lrp5 gene on bone biomechanical properties, J. Bone Miner. Res. 17 (2002) M163.

[24]. Robinson JA, et al. , Wnt/β-catenin signaling is a Normal physiological response to mechanical loading in bone, J. Biol. Chem. 281 (2006) 31720–31728. [PubMed: 16908522]

[25]. Bonewald LF, Johnson ML, Osteocytes, mechanosensing and Wnt signaling, Bone 42 (2008) 606–615. [PubMed: 18280232]

[26]. Burger EH, et al. , Function of osteocytes in bone - their role in mechanotransduction, J. Nutr. 125 (1995) 2020S–2023S. [PubMed: 7602386]

[27]. Lanyon LE, Control of bone architecture by functional load bearing, J. Bone Miner. Res. 7 (1992) S369–S375. [PubMed: 1485545]

[28]. Lara-Castillo N, et al. , In vivo mechanical loading rapidly activates beta-catenin signaling in osteocytes through a prostaglandin mediated mechanism, Bone 76 (2015) 58–66. [PubMed: 25836764]

[29]. Ajubi NE, et al. , Pulsating fluid flow increases prostaglandin production by cultured chicken osteocytes - a cytoskeleton - dependent process, Biochem. Biophys. Res. Commun. 225 (1996) 62–68. [PubMed: 8769095]

[30]. Genetos DC, et al. , Oscillating Fuid flow activation of gap junction Hemichannels induces ATP release from MLO-Y4 osteocytes, J. Cell. Physiol. 212 (2007) 207–214. [PubMed: 17301958]

[31]. Kamel MA, et al. , Activation of beta-catenin signaling in MLO-Y4 osteocytic cells versus 2T3 osteoblastic cells by fluid flow shear stress and PGE(2): implications for the study of mechanosensation in bone, Bone 47 (5) (2010) 872–881. [PubMed: 20713195]

[32]. Xia X, et al. , Prostaglandin promotion of osteocyte gap junction function through transcriptional regulation of connexin 43 by glycogen synthase kinase 3/beta-catenin signaling, Mol. Cell. Biol. 30 (1) (2010) 206–219. [PubMed: 19841066]

[33]. Armstrong VJ, et al. , Estrogen receptor α is required for strain-related β-catenin signaling in osteoblasts, J. Bone Miner. Res. 22 (Suppl. 1) (2007) S95 (abstr S064).

[34]. Kitase Y, et al. , Mechanical induction of PGE(2) in osteocytes blocks glucocorticoid induced apoptosis through both the beta-catenin and PKA pathways, J. Bone Miner. Res. 25 (12) (2010) 2657–2668. [PubMed: 20578217]

[35]. Pavalko FM, et al. , Fluid shear-induced mechanical signaling in MC3T3-E1 osteoblasts requires cytoskeleton-integrin interactions, Am. J. Phys. 275 (C) (1998) C1591–C1601.

[36]. Batra N, et al. , Mechanical stress-activated integrin α5β1 induces opening of connexin 43 hemichannels, Proc. Natl. Acad. Sci. USA. 109 (2012) 3359–3364. [PubMed: 22331870]

[37]. Wang Y, et al. , A model for the role of integrins in flow induced mechanotransduction in osteocytes, Proc. Natl. Acad. Sci. U. S. A. 104 (2007) 15941–15946. [PubMed: 17895377]

[38]. Ypey DL, et al. , Voltage, calcium, and stretch activated ionic channels and intracellular calcium in bone cells, J. Bone Miner. Res. 7 (Suppl. 2) (1992) S377. [PubMed: 1283043]

[39]. Li J, et al. , L-type calcium channels mediate mechanically induced bone formation in vivo, J. Bone Miner. Res. 17 (10) (2002) 1795–1800. [PubMed: 12369783]

[40]. Santos A, et al. , Early activation of the beta-catenin pathway in osteocytes is mediated by nitric oxide, phosphatidyl inositol-3 kinase/Akt, and focal adhesion kinase, Biochem. Biophys. Res. Commun. 391 (1) (2010) 364–369. [PubMed: 19913504]

[41]. Case N, et al. , Beta-catenin levels influence rapid mechanical responses in osteoblasts, J. Biol. Chem. 283 (43) (2008) 29196–29205. [PubMed: 18723514]

[42]. Alford A, Jacobs C, Donahue H, Ocillating fluid flow regulates gap junction communication in osteocytic MLO-Y4 cells by an ERK1/2 MAP kinase -dependent mechanism, Bone 33 (2003) 64–70. [PubMed: 12919700]

[43]. Kyono A, et al. , FGF and ERK signaling coordinately regulate mineralization-related genes and play essential roles in osteocyte differentiation, J. Bone Miner. Metab. 30 (2012) 1–12. [PubMed: 22167381]

[44]. Jahn K, et al. , Skeletal muscle secreted factors prevent glucocorticoid-induced osteocyte apoptosis through activation of beta-catenin, European Cells Mater. 24 (2012) 197–209 (discussion 209–10).

[45]. Park KH, et al. , Ex vivo assessment of contractility, fatigability and alternans in isolated skeletal muscles, J. Vis. Exp. 69 (2012) e4198.

[46]. DasGupta R, Fuchs E, Multiple roles for activated LEF/TCF transcription complexes during hair follicle development and differentiation, Development 126 (20) (1999) 4557–4568. [PubMed: 10498690]

[47]. Warner SE, et al. , Botox induced muscle paralysis rapidly degrades bone, Bone 38 (2) (2006) 257–264. [PubMed: 16185943]

[48]. Stone AV, et al. , Effects of Botox and Neuronox on muscle force generation in mice, J. Orthop. Res. 25 (12) (2007) 1658–1664. [PubMed: 17600825]

[49]. Kato Y, et al. , Establishment of an osteocyte-like cell line, MLO-Y4, J. Bone Miner. Res. 12 (1997) 2014–2023. [PubMed: 9421234]

[50]. Cai C, et al. , MG53 nucleates assembly of cell membrane repair machinery, Nat. Cell Biol. 11 (1) (2009) 56–64. [PubMed: 19043407]

[51]. Zhao X, et al. , Compromised store-operated Ca^{2+} entry in aged skeletal muscle, Aging Cell 7 (4) (2008) 561–568. [PubMed: 18505477]

[52]. Shen J, et al. , Deficiency of MIP/MTMR14 phosphatase induces a muscle disorder by disrupting Ca(2+) homeostasis, Nat. Cell Biol. 11 (6) (2009) 769–776. [PubMed: 19465920]

[53]. Nosek TM, et al. , Functional properties of skeletal muscle from transgenic animals with upregulated heat shock protein 70, Physiol. Genomics 4 (1) (2000) 25–33. [PubMed: 11074010]

[54]. Noursadeghi M, et al. , Quantitative imaging assay for NF-kappaB nuclear translocation in primary human macrophages, J. Immunol. Methods 329 (1–2) (2008) 194–200. [PubMed: 18036607]

[55]. Labarca C, Paigen K, A simple, rapid, and sensitive DNA assay procedure, Anal. Biochem. 102 (2) (1980) 344–352. [PubMed: 6158890]

[56]. Pirazzini M, et al. , Botulinum neurotoxins: biology, pharmacology, and toxicology, Pharmacol. Rev. 69 (2) (2017) 200–235. [PubMed: 28356439]

[57]. Gehling AM, et al. , Evaluation of volume of intramuscular injection into the caudal thigh muscles of female and male BALB/c mice (*Mus musculus*), J. Am. Assoc. Lab. Anim. Sci. 57 (1) (2018) 35–43. [PubMed: 29402350]

[58]. Tang-Liu DD, et al. , Intramuscular injection of 125I-botulinum neurotoxin-complex versus 125I-botulinum-free neurotoxin: time course of tissue distribution, Toxicon 42 (5) (2003) 461–469. [PubMed: 14529727]

[59]. Qin YX, Lam H, Intramedullary pressure and matrix strain induced by oscillatory skeletal muscle stimulation and its potential in adaptation, J. Biomech. 42 (2) (2009) 140–145. [PubMed: 19081096]

[60]. Lam H, Qin YX, The effects of frequency-dependent dynamic muscle stimulation on inhibition of trabecular bone loss in a disuse model, Bone 43 (6) (2008) 1093–1100. [PubMed: 18757047]

[61]. Swift JM, et al. , Simulated resistance training during hindlimb unloading abolishes disuse bone loss and maintains muscle strength, J. Bone Miner. Res. 25 (3) (2010) 564–574. [PubMed: 19653816]

[62]. Javaheri B, et al. , Deletion of a single beta-catenin allele in osteocytes abolishes the bone anabolic response to loading, J. Bone Miner. Res. 29 (3) (2014) 705–715. [PubMed: 23929793]

[63]. Bonewald L, Use it or lose it to age: a review of bone and muscle communication, Bone 120 (2019) 212–218. [PubMed: 30408611]

[64]. Hamrick MW, The skeletal muscle secretome: an emerging player in muscle-bone crosstalk, Bonekey Rep. 1 (2012) 60. [PubMed: 23951457]

[65]. Herrmann M, et al. , Interactions between muscle and bone-where physics meets biology, Biomolecules 10 (3) (2020).

[66]. Norvell SM, et al. , Fluid shear stress induces β-catenin signaling in osteoblasts, Calcif. Tissue Int. 75 (2004) 396–404. [PubMed: 15592796]

[67]. Lau KH, et al. , Up-regulation of the Wnt, estrogen receptor, insulin-like growth factor-I, and bone morphogenetic protein pathways in C57BL/6J osteoblasts as opposed to C3H/HeJ osteoblasts in part contributes to the differential anabolic response to fluid shear, J. Biol. Chem. 281 (14) (2006) 9576–9588. [PubMed: 16461770]

[68]. Sunters A, et al. , Mechano-transduction in osteoblastic cells involves strain-regulated estrogen receptor alpha-mediated control of insulin-like growth factor (IGF) I receptor sensitivity to ambient IGF, leading to phosphatidylinositol 3-kinase/AKT-dependent Wnt/LRP5 receptor-independent activation of beta-catenin signaling, J. Biol. Chem. 285 (12) (2010) 8743–8758. [PubMed: 20042609]

[69]. Kamel MA, Holladay BR, and Johnson ML, Potential interaction of prostaglandin and Wnt signaling pathways mediating bone cell responses to fluid flow. J J. Bone Miner. Res, 2006. 21 (suppl 1): p. S92 (abs F166).

[70]. Staudt LM, Gene expression profiling of lymphoid malignancies, Annu. Rev. Med. 53 (2002) 303–318. [PubMed: 11818476]

[71]. Lara N, et al. , Bone-muscle crosstalk is demonstrated by morphological and functional changes in skeletal and cardiac muscle cells in response to factors produced by MLO-Y4 osteocytes, J. Bone Miner. Res. 25 (Suppl. 1) (2010) S112 (abstract FR0282).

[72]. Marotti G, et al. , Structure: function relationships in the osteocyte, Ital. J. Min. Electrolyte Metab. 35 (1990) 707–715.

[73]. Lang T, et al. , Sarcopenia: etiology, clinical consequences, intervention, and assessment, Osteoporos. Int 21 (4) (2010) 543–559. [PubMed: 19779761]

[74]. Sample SJ, et al., JBMR, 2008.

[75]. Bain SD, et al. , Neuromuscular dysfunction, independent of gait dysfunction, modulates trabecular bone homeostasis in mice, J. Musculoskelet. Neuronal Interact. 19 (1) (2019) 79–93. [PubMed: 30839306]

[76]. Macias BR, Aspenberg P, Agholme F, Paradoxical Sost gene expression response to mechanical unloading in metaphyseal bone, Bone 53 (2) (2013) 515–519. [PubMed: 23337040]

[77]. Blecher R, et al. , New functions for the proprioceptive system in skeletal biology, Philos. Trans. R. Soc. Lond. B Biol. Sci. 373 (1759) (2018).

[78]. Herber CB, et al. , Estrogen signaling in arcuate Kiss1 neurons suppresses a sexdependent female circuit promoting dense strong bones, Nat. Commun. 10 (1) (2019) 163. [PubMed: 30635563]

[79]. Farman HH, et al. , Female mice lacking estrogen receptor-α in hypothalamic proopiomelanocortin (POMC) neurons display enhanced estrogenic response on cortical bone mass, Endocrinology 157 (8) (2016) 3242–3252. [PubMed: 27254004]

[80]. Holguin N, Brodt MD, Silva MJ, Activation of Wnt signaling by mechanical loading is impaired in the bone of old mice, J. Bone Miner. Res. 31 (12) (2016) 2215–2226. [PubMed: 27357062]

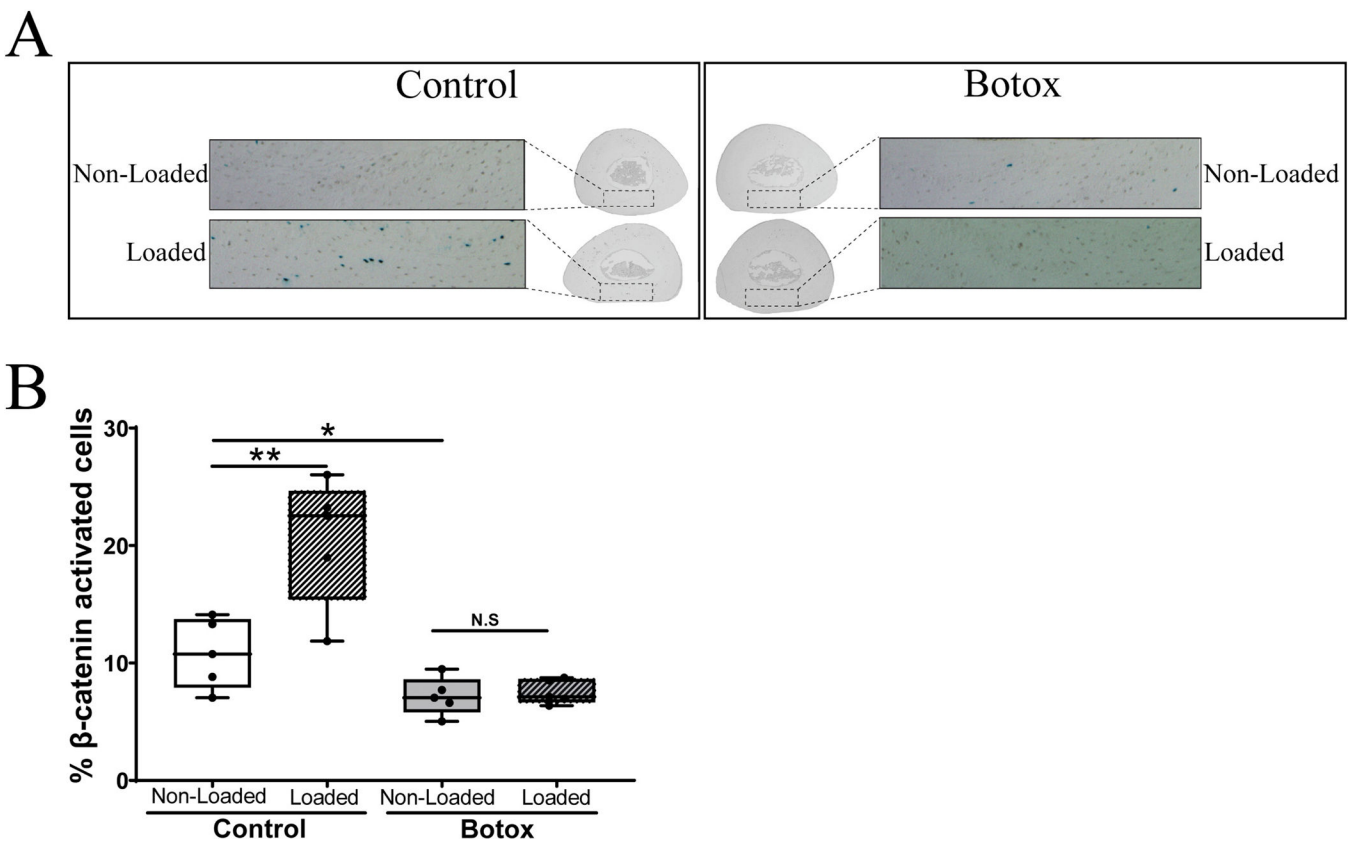

Fig. 1.

Effect of muscle paralysis on loading-activated Wnt/β-catenin activation. We injected Botox®, 1 unit per hindlimb (n = 5) or PBS (n = 5) in muscles rounding the right tibia of TOPGAL mice 3 days prior to in vivo loading. The right tibia of all animals was subjected to a single cyclical loading session (~2600με, 2 Hz, 0.1 s insertion, 100 cycles) (labeled as Loaded). Non-Loaded left tibia of each animal was used as internal control. Animals returned to normal cage activity. Hindlimbs were collected 24 h post loading, fixed, stained, sectioned, and counted as previously published. DAPI staining was used to determine total number of cells in the cross-section. (A) Representative images of cross-sectional area of interest. (B) Bar graphs representing the percentage of activated cells per region of interest. A Paired *t*-test was used to establish statistical significance. *$p < 0.05$, N.S. = no statistical significance was found.

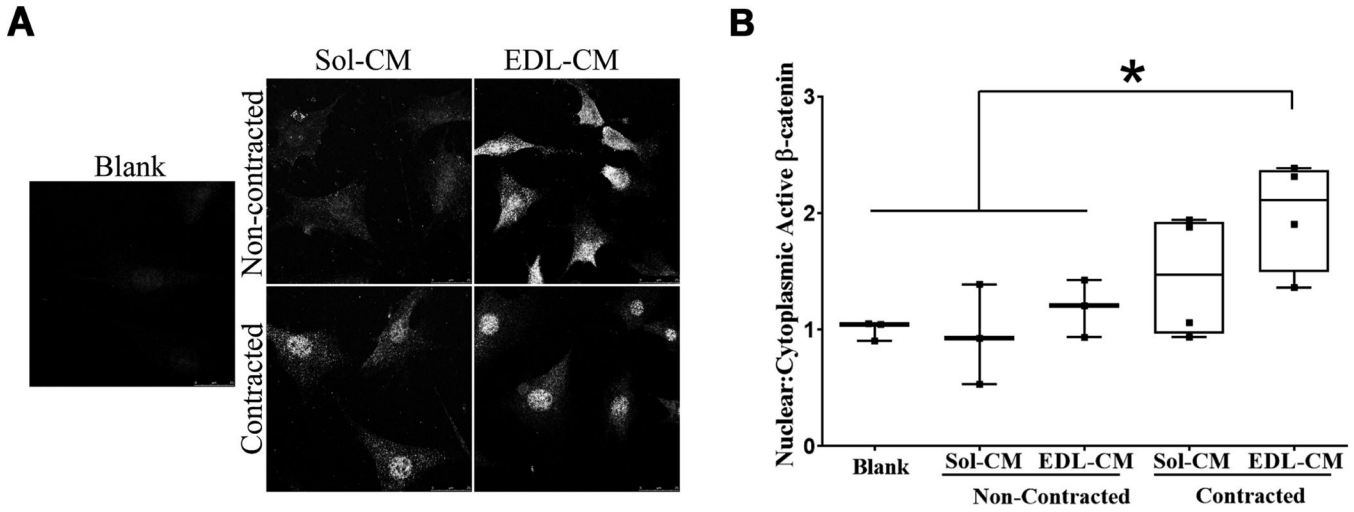

Fig. 2.

Conditioned media from contracted EDL, but not Soleus, muscle induces nuclear translocation of β-Catenin MLO-Y4 osteocyte-like cells. We contracted isolated muscles, ex vivo, Soleus (Sol) and EDL from 5 to 7 month-old male mice. We collected this media and incubated MLO-Y4 osteocyte at a final 10 % concentration for 2 h. MLO-Y4 cells were then fixed and incubated with antibody against β-catenin. (A) representative images of MLO-Y4 cells when exposed to different media. (B) Nuclear to cytoplasmic ratio was calculated using ImageJ from at least 50–75 cells obtained from 5–6 different fields in each condition with a total of 50–75 cells counted. Bars represent mean ± std. deviation from at least 3 independent studies. A one way ANOVA was performed to differences in groups $F(4,12) = p = 0.03$. A LSD posthoc test was performed to determine statistical differences among the different groups $^*p < 0.05$.

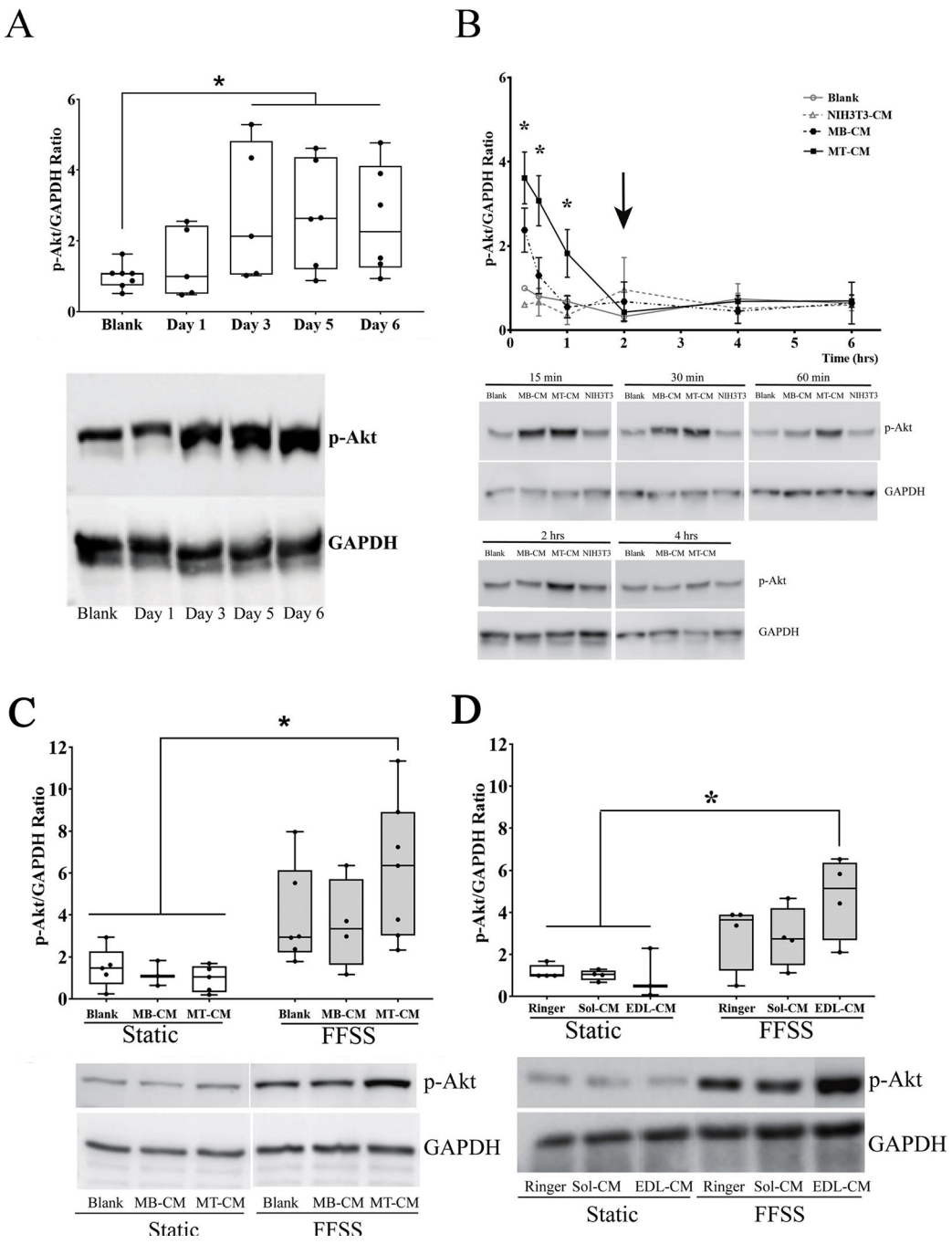

Fig. 3.

Effect of secreted factors from different stages of muscle cell differentiation and ex-vivo contracted muscles on activation of the PI3K/Akt pathway in MLO-Y4 cells. (A) C2C12 myoblast cells were differentiated into myotubes by addition of differentiating media (2.5 % horse serum containing DMEM) for six days. Media was exchanged daily and collected at days 1, 3, 5, and 6 after differentiation began. MLO-Y4 cells were incubated with 10 % blank or C2C12 cell conditioned media (CM) for 30 min. Western blotting was performed to detect pAkt and GAPDH (to normalize data). Densitometric quantitation and analysis of

the bands was performed. Graph represents the ratio between the phosphorylated form of Akt and GAPDH. Bars indicate mean ± SD (n = 5–7). A Kruskal-Wallis H Test was used to determine if there was any difference among the different groups with performed and Dunn's procedure with a Bonferroni correction for multiple comparisons. $H^2(3) = 20.810$, $p < 0.001$. (B) Time course phosphorylation of Akt when MLO-Y4 cells were incubated with 10 % blank media or NIH3T3-CM, C2C12 myoblast-CM (MB-CM) or myotube-CM (MT-CM) for different time points. Arrow points to the time point when phosphorylated Akt returns to basal levels. Graph represents the mean ± SEM of the ratio of the density of the bands (n = 2–6). ANOVA at each single time point was run to obtain cell line effect on phosphorylation of Akt *$p < 0.05$ myotube CM vs blank treated cells; $^{\#}p < 0.05$ myotube CM treated cells vs NIH3T3 CM (**C**) MLO-Y4 cells were subjected to FFSS for 2 h in the presence of C2C12 CM or contracted muscle CM. A one way ANOVA test was performed on transformed data $F(5,24) = 6.387$ n = 3–7, $p < 0.001$ An LSD posthoc analysis was used to determine significance. (D). Graph represents the ratio of the phosphorylated form of Akt to GAPDH (mean ± SD), (n = 3–8). A Kruskal-Wallis Test was performed to assess for differences between groups $H^2(5) = 12.189$, $p = 0.032$. A Bonferroni correction was used to account for multiple comparisons *$p < 0.017$.

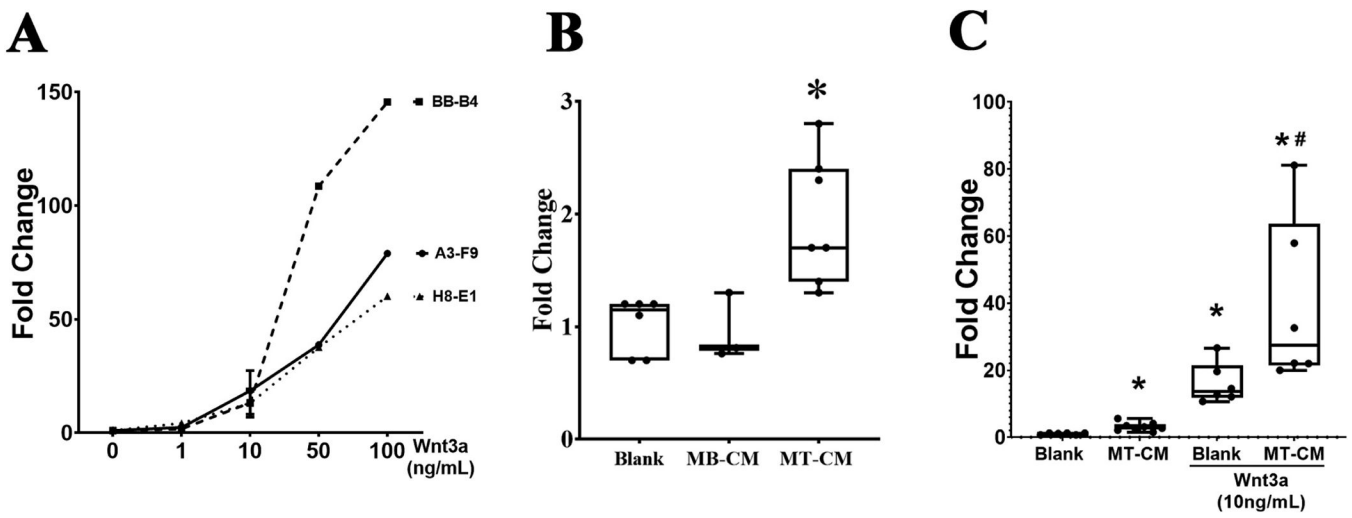

Fig. 4.

Development and testing of TOPflash-MLO-Y4 cells. (A) MLO-Y4 cells were stably transfected using Luc2P/LEF-Hygro Promega vector. After several rounds of selection, 3 clonal cell lines were identified and tested. Three clonal cell lines were identified, BB-B4, A3-F9 and H8-E1. Cells were incubated with different concentrations of Wnt3a for 24 h and luciferase activity was measured. (B) A3-F9 cells were incubated for 24 h with conditioned media from C2C12 in the myoblast (MB-CM) or myotube (MT-CM) state. Graph represent ratio of luciferase activity against blank. A one way ANOVA test was performed using the Log10 transformed data $F(2,10) = 6.870$, $p = 0.013$. An LSD posthoc test was used to compare different groups. *$p < 0.05$ different from other groups. (C) A3-F9 cells were incubated for 24 h with MT-CM in the presence or absence of submaximal concentration of Wnt3a (10 ng/ml). Bars represent mean ± standard deviations. Data was transformed using a Log10 transformation in order to meet the assumption for parametric tests. After transformation, a one-way ANOVA was performed $F(3,22) = 90.441$, $p < 0.001$, followed a LSD posthoc test in order to compare different groups. *$p < 0.05$.

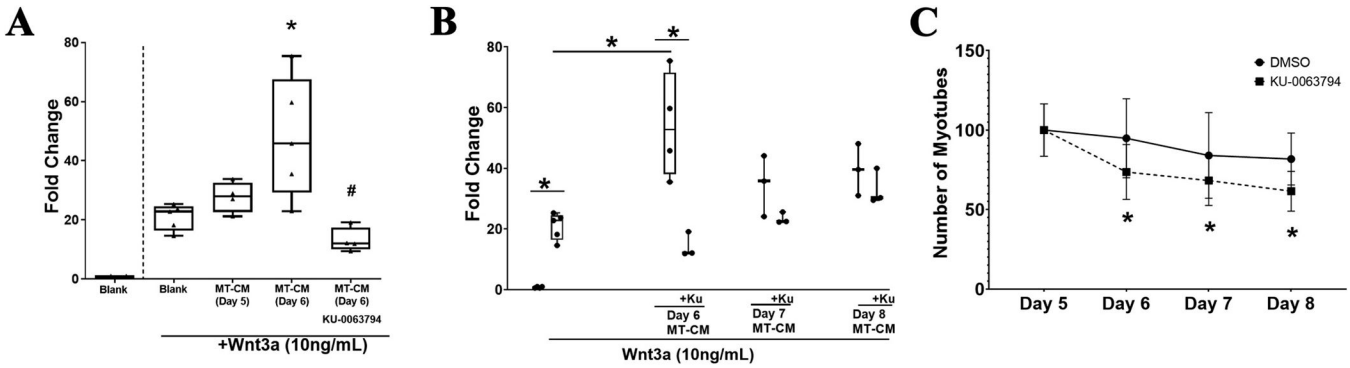

Fig. 5.

mTOR pathway is involved in the production of muscle derived factors. (A) TOPflash-MLO-Y4 cells (A3-F9) were incubated for 24 h with 10 ng/ml Wnt3a ± 10 % of MT-CM from days 5 or day 6 ± 10 μM mTOR inhibitor, KU-0063794. Bars represent fold change of luciferase activity compared to Blank without Wnt3a treatment (not shown in the graph). Transformed data (using Log10) was normally distributed assessed by Shapiro-Wilk test and had Homogeneity of Variances as assed by the Levene's Test ($p = 0.302$). A one-way ANOVA was performed on transformed data to determine the effect of mTOR pathway inhibition on production of muscle conditioned media. $F(3,14) = 11.927$, $p < 0.001$. An LSD posthoc test was applied for multiple comparisons *$p < 0.05$ against blank + Wnt3a, $^{\#}p < 0.05$ against MT-CM Day 6 without inhibitor ($n = 4–5$ per group, with a minimum of 3 replicates per experiment). (B) C2C12 cells were differentiated into myotubes. On day 5, cells were incubated in the presence or absence of mTOR inhibitor for 24 h and media was removed. We collected media on day 6, 7 and 8 and add fresh media to the culture. TOPflash-MLO-Y4 cells (A3-F9) were incubated with different conditioned media for 24 h. Luciferase activity was then measured and plotted as fold change against blank. Data were transformed data (using Log10) and a Student *t*-test was used to compared the effect of the mTOR inhibitor. *$p < 0.05$, N.S. = non significant ($n = 3–4$ per group, with a minimum of 3 replicates per experiment). (C) Quantitation of number of myotubes per area of interest. Per treatment ($n = 3–4$) per condition.